

# Antenna Optimization for Vehicular Environments

Sai Ananthanarayanan P.R., Cynthia M. Furse

Electrical and Computer Engineering (ECE)

University of Utah (U of U)

Salt Lake City, Utah

[saianantha21@gmail.com](mailto:saianantha21@gmail.com)

[cfurse@ece.utah.edu](mailto:cfurse@ece.utah.edu)

**Abstract**— This paper presents a multi-antenna optimization for communication in a Rockwell T-39 Sabreliner, a mid-size aircraft with a metallic body. The aircraft channel at 2.45 GHz is modeled using site specific 3D ray-tracing software. Added effects from system details including the antenna radiation patterns, mutual coupling, etc. are incorporated into a network theory based detailed signal model. The paper considers traditional antennas including dipoles, square patches, PIFAs, and polarization agile patches along with some more complex shaped patches and PIFAs. A random search algorithm was used to optimize capacity for arrays with widely divergent element count, element type, matching, directivity, polarization alignment, efficiency, spatial correlation and coupling. The polarization agile patch provides the best capacity for locations near the aircraft ceiling while the PIFAs with more variety in shape (spiral shapes) provide the best capacity for locations near the floor. This is because the signals reaching the roof and sides contain more polarization diversity than those in the center of the body where the nonconductive floor is located.

**Keywords-component; aircraft communication, antenna optimization, 3D ray-tracing)**

## I. INTRODUCTION

Aircraft health monitoring is of the utmost importance for today's aging aircraft fleets. Existing planes are being retrofitted with sensors for electrical faults, engine wear, chemical and corrosion problems, moisture, temperature, vibration, etc. and new planes are being built with many of these sensors already integrated into their monitoring systems. Running wires for all of these sensors adds weight and failure points, in which can be reduced by using wireless sensor networks.

Wireless communication in aircraft is challenging because of the multipath reflections caused by the closed metallic structure, significant loss from tightly packed bodies and a broad band noise channel caused by a plethora of existing avionics, radar, etc. This multipath channel in aircraft is much more complex than the usual indoor/outdoor channels [1][2]. One of the potential methods of increasing the communication capacity in a rich multipath environment such as aircraft is to use multiple antennas. The potential capacity is dependent on the channel properties including the path loss, angle of arrival, angle of departure, and also on the antenna and its front end properties including matching, losses, radiation pattern, etc. The objective of this paper is to optimize multi-antenna array designs to take advantage of the unique site-specific multipath changes at different locations within the aircraft and to determine if each location requires an

individual antenna design or if collective regions within the aircraft can make use of a similar design thus reducing the overall design cost for the system.

In order to optimize a wide variety of antennas at specific sites within the aircraft, the unique channel at each location was predicted using a site specific 3D ray-tracing model [3]-[5] **Error! Reference source not found.** This paper studies antenna optimization on a mid-size aircraft Rockwell T-39 Sabreliner. The 3D simulations were run on 34 different antenna locations in the aircraft. The receivers were placed on the floor and the sealing of the aircraft to study the effects of both single and dual polarized antennas. The antenna and front end effects are added to the 3D ray tracing model using a network-theory based detailed signal model that includes the antenna polarization, matching, losses, radiation pattern, efficiency, and antenna gain. Section II describes this detailed modeling that was done at 2.45 GHz for a Rockwell T-39 Sabreliner mid-sized commuter aircraft with a metallic body.

The goal of this paper is to optimize antennas for site-specific locations within the aircraft and determine the level of uniqueness required in the design at different locations. But truly optimizing for any possible design is too costly. Instead, a selection of antennas chosen to have a broad range of radiation patterns, polarizations and cross-coupling characteristics was chosen, and the optimization was narrowed to this selection of antenna types. Arrays of 4 input and 4 output (4x4) antennas were selected from patch, monopoles above a ground plane, planar spirals, patches, and planar inverted F antennas (PIFAs), agile patches and PIFAs, and a U-T-A-H combination of microstrip antennas were optimized at 2.45 GHz for specific sites within the aircraft. Section IV describes these antennas and their characteristics. The details of the random search method used to optimize the multi-antenna arrays and the results are described in Section V.

## II. 3D RAY-TRACING

A highly efficient 3D ray-tracing model is used. This method is based on a triangular grid method that minimizes computational time by determining which rays arrive at the receive antenna without having to test whether they bounced off every wall in the aircraft. The algorithm uses 30% or less CPU time than other ray-tracing methods and has been validated in 2D indoor and outdoor environments. The output of the 3D ray-tracing software includes received power, path gains, complex electric fields and angle of arrival and departure (AOA/AOD) information that can be used to

estimate site-specific capacity performance within the enclosed environment.

For this paper, rectangular facets have been used to represent the simple surfaces such as walls and obstacles found in the Rockwell T-39 Sabreliner. It is simulated with 15 faceted sides to represent the cylindrical shape of the fuselage, and flat rectangular surfaces for the front and back of the fuselage. For simplification, the floor was assumed to be electrically transparent for 2.45 GHz used in 802.11 communication. Both lossy and reflective internal obstacles such as chairs, reflective walls, etc. were included in the model. All aircraft walls were assumed to be perfect electrical conductors (PEC). Glass windows were also included in the model. Chairs were modeled as two flat surfaces with a loss factor of 0.1 dB connected at one edge, based on our transmission measurements of an individual chair made in an anechoic chamber. Lossy walls within the cabin were modeled as a rectangular surface with a loss factor of 2.8 dB, which was found empirically by comparing simulated and measured values with different loss factors for the walls. Antenna locations were kept a 0.1 m (0.82 wavelengths at 2.45 GHz) from walls to minimize modeling errors.

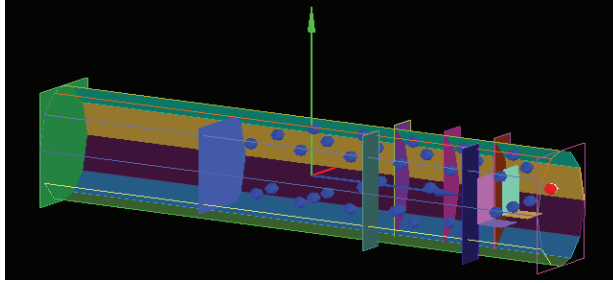


Figure 1: The figure shows the Rockwell T-39 Sabreliner with transmitter placed in the front dash board as shown by the red dot and 34 receivers placed throughout the cabin as shown by blue dots.

The transmitters were fixed as 4 vertically polarized quarter wavelength monopole antennas over a ground plane placed on the dashboard in the front of the aircraft. The receivers were placed throughout the aircraft and are shown in figure 1. At each location 100 simulations were performed by moving the four receiver antennas over a grid of 20 cm X 20 cm. The 3D ray tracer outputs the complex electric fields and angle of arrival and departure for each transmitter – receiver antenna pair. These results were compiled into the channel matrix  $\mathbf{H}$ , which was then used to calculate capacity. The complete channel model including the front end effects can be written as:

$$\mathbf{H} = Z_0^{1/2} \underbrace{\mathbf{S}_{21} (\mathbf{I} - \mathbf{S}_{RR} \mathbf{S}_{11})^{-1}}_{\mathbf{M}_R} \left( \mathbf{I} + \frac{\mathbf{Z}_{RR}}{Z_0} \right)^{-1} \underbrace{\mathbf{E}_{cdr}}_{\text{rad eff}} \underbrace{\mathbf{H}_{3D}}_{H_{DP}} \underbrace{\mathbf{E}_{cdt}}_{\text{rad eff}} \underbrace{(\mathbf{I} - \mathbf{S}_{TT})}_{\mathbf{M}_T}, \quad (1)$$

where  $Z_0$  is the characteristic impedance of the feed,  $\mathbf{S}_{TT}$  and  $\mathbf{S}_{RR}$  are the scattering parameters of the unloaded transmit and receive arrays respectively,  $\mathbf{S}_{RT}$  is the channel scattering matrix, and  $\mathbf{S}_{11}$  and  $\mathbf{S}_{21}$  represent a matching circuit and transmission circuit for the selected antenna matching approach. The channel matrix  $\mathbf{H}$  also includes directivity ( $\mathbf{D}_R$ ),

polarization ( $\mathbf{P}$ ), efficiency at both transmitter ( $\mathbf{E}_{cdt}$ ) and receiver ( $\mathbf{E}_{cdr}$ ), matching at transmitter ( $\mathbf{M}_T$ ), and receiver ( $\mathbf{M}_R$ ). The system capacity is obtained as:

$$C = \log_2 \det[\mathbf{I} + \text{SNR} \mathbf{H}_n \mathbf{H}_n^H] \quad (2)$$

### III. ANTENNA OPTIMIZATION

This section describes the optimization algorithm used to select a set of receiver antennas from the list in the previous section, and combine them into the most effective multi-antenna system they can provide for a specific location in the

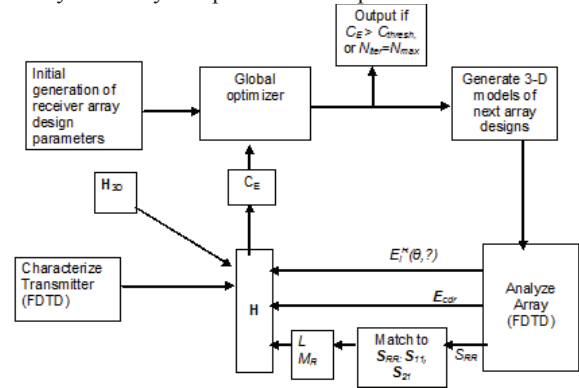


Figure 2: Optimization Flowchart

aircraft. Dipoles, patch, spiral, PIFA, and agile patch, antennas were designed at 2.45 GHz as described above. 720 permutations of these antennas were used for the random search algorithm shown in Figure 2. An antenna type is selected from the list above and individually optimized in CST Microwave Studio to have 50 ohm impedance match. The matrix of radiation efficiencies,  $\mathbf{E}_{cdr}$ , and a matrix of array input port efficiencies,  $\mathbf{Z}_{RR}$ , with corresponding  $S$ -parameter formulation,  $\mathbf{S}_{RR}$  are obtained from CST Microwave studio. Given  $\mathbf{S}_{RR}$ , one can choose a matching strategy and obtain  $S$ -parameters describing the matching network,  $\mathbf{S}_{11}$  and  $\mathbf{S}_{21}$ . These allow for the computation of a receiver matching term,  $\mathbf{M}_R$ . The 3D ray tracing algorithm described in Section II is used for computing the channel characteristics.

### IV. ANTENNAS

Numerous regular arrays including uniform planar, linear, and circular arrays involving dipoles/monopoles or patches have been considered in the literature for wireless sensor and handheld applications. For this paper, we consider quarter wave monopoles over a ground plane, spirals, patches, polarization agile patch [5], and UTAH antenna at 2.45 GHz. Unless otherwise stated, the substrate used for all the designs is air. With the Rogers 4003C substrate with  $\epsilon_r$  of 3.48, we can achieve a smaller size of the patches and UTAH antennas. This section briefly describes the spirals, U logo and the UTAH antenna.

#### A. Spiral Antenna

Figure 3 shows the two spiral antennas considered in this paper. The spiral 1 antenna has a dimension of 46 X 15 X 5

mm. The feed and short points are separated by 4 mm. The spiral 2 antenna has a dimension of 36 X 15 X 5 mm. The feed and short points are separated by 8 mm. Both were simulated in CST with a ground plane of 50 mm X 50 mm and with air substrate.

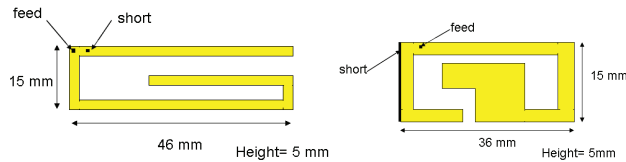


Figure 3. Spiral antennas a) Spiral antenna 1 operating at 2.45 GHz. b) Spiral antenna 2

The radiation patterns are shown in Figure 8.3 and Figure 8.4, respectively, with gains of 4.7 and 3.4 dB. These antennas are particularly well-suited to the tight spaces in the aircraft environment because of their compact size.

### B. U logo Antenna

Figure 4 shows the University of Utah logo antenna which is in the form of a PIFA. This antenna has a dimension of 35mm X 35 mm X 5 mm. The antenna is well matched at 2.45 GHz with a return loss of -27 dB. The feed and short positions are as shown in Figure 4. The position of the feed and short were chosen by simulations performed in CST Microwave Studio to provide the best match at 2.45 GHz and also for providing best directivity. The ground plane had a dimension of 40 mm X 40 mm and air dielectric was assumed for simulation.

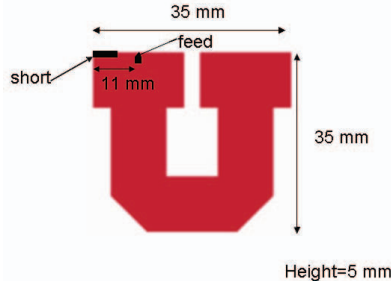


Figure 4. A PIFA antenna designed in the form of University of Utah radiating at 2.45 GHz.

### C. UTAH Antenna

Figure 5 shows the UTAH antenna, which is a set of patches above a ground plane. The UTAH antenna consists of U, T, A, and H antennas each individually matched at 2.45 GHz. It can be used as individual antenna elements, or grouped together. The total dimension of the UTAH antenna is 182mm X 40 mm. The T-antenna has a bandwidth of 500 MHz.

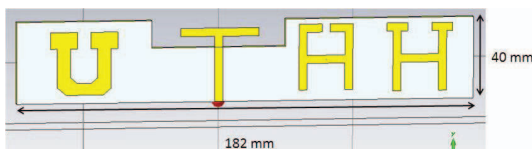


Figure 5. UTAH Antenna

## V. RESULTS

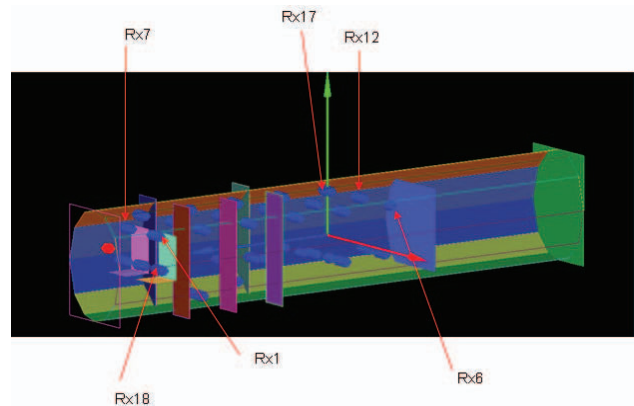


Figure 6. Simulation locations of transmitter and receiver in Rockwell T-39 Sabreliner fuselage.

Eight antennas have been used for analyzing multi antenna communication in aircraft. These include dipoles (monopole over ground plane), patch, PIFA, Spiral1, Spiral 2, U logo, UTAH antenna and polarization agile patch. The substrate for all the antennas except the PIFAs and Spiral was assumed to be Roger 4003C with permittivity of 3.48 and a loss tangent of 0.0035.

The transmitter antenna was a 2.45 GHz dipole. The antenna parameters such as gain, efficiency, matching, polarization etc. were included in the channel simulations performed using the 3D ray-tracing model. The complete channel matrix  $\mathbf{H}$  was obtained as in (1). This channel matrix was normalized and the capacity was calculated using (2) for SNR estimated using [6]. The measurement locations in the fuselage of the Rockwell T-39 Sabreliner are shown in Figure 6. Rx1-Rx17 are placed in the ceiling of the aircraft while Rx18-Rx34 are placed in the floor and the front chairs.

At each of the receiver locations, 100 simulations were run by moving the receiver in a 10X10 grid with each measurement separated by 0.01 m. First we will plot the capacity obtained using 4 dipole antennas at the transmitter and by using 4 antennas of the same type at receiver (for eg. 4 agile patches, 4 U logo etc). Figure 7 shows the average, maximum, and minimum capacity for each of the antenna combinations at locations Rx1-Rx17 in the roof of the aircraft. From Figure 7, we observe that for the receivers placed on the roof of the aircraft, the polarization agile patch antenna provides the best capacity estimate, followed by the UTAH antenna and the U logo antenna. This shows that there is polarization misalignment for the signals reaching the rooftop and the dual polarized antenna takes into account the lost energy, thus increasing the capacity.

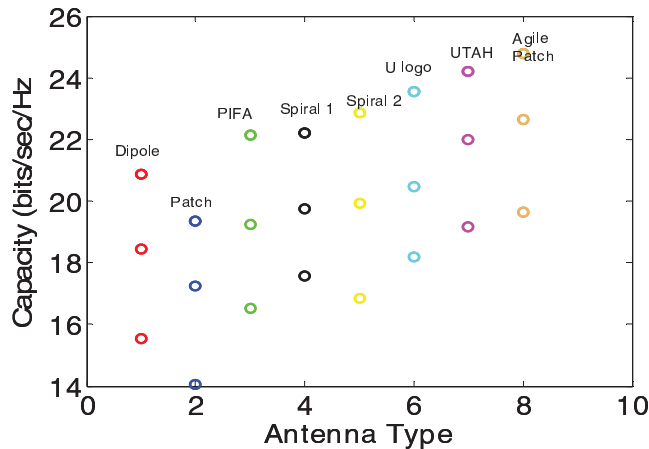


Figure 7: Minimum, maximum, and average capacity plot for the Rockwell T-39 channel simulated using the 3D ray-tracing model for receiver locations Rx1-Rx17

Similarly, by plotting the average, maximum, and minimum capacity for each of the antenna combinations for receiver locations Rx18-Rx34 located on the floor and chairs of the aircraft we observe that the UTAH antenna and the U logo antenna provide better capacity estimates as compared to the other antennas. This shows that vertical polarized antennas perform better than dual polarized antennas when the sensors are placed in the floor.

Next we plot the capacity obtained using 4 dipole antennas at the transmitter and 4 other antennas with different antenna combinations (like 2 agile patch+2 spirals, etc.) at the receiver. Figure 8 plots the average, maximum, and minimum capacity for each of the antenna combinations. From Figure 8, we observe that for the receivers placed on the floor and the chairs of the aircraft, the UTAH antenna and the U logo antenna provide better capacity estimates as compared to the other antennas. Similarly by plotting the average, maximum, and minimum capacity for each of the antenna combinations for receiver locations Rx1-Rx17 located along the ceiling of the aircraft we observe that the polarization agile patch antenna provides the best capacity estimate followed by the UTAH antenna and the 2 spiral 2 + 2 agile patch combination. This shows that there is polarization misalignment for the signals reaching the rooftop and the dual polarized antenna takes into account the lost energy, thus increasing the capacity.

## I. CONCLUSION

This paper presents a multi antenna optimization technique for aircraft sensors. The site-specific 3D ray-tracing model is used to analyze a multi antenna system in a Rockwell T-39 Sabreliner which is a midsize aircraft with metallic body. Well-known antennas including dipoles, patches, PIFAs, and the polarization agile patch are used for performing multi antenna optimization. Along with these, two spiral antennas, the University of Utah logo antenna and the UTAH antenna have been designed in the paper. The antennas are matched for operating at 2.45 GHz. The multi antenna optimization was

performed with capacity as the cost function. It was observed that for the antennas placed on the aircraft rooftop and on the sides, the polarization agile patch antenna provided optimum capacity, followed by the UTAH antenna. This was due to the fact that the signals reaching the rooftops and sides have both vertical and horizontal polarization components.

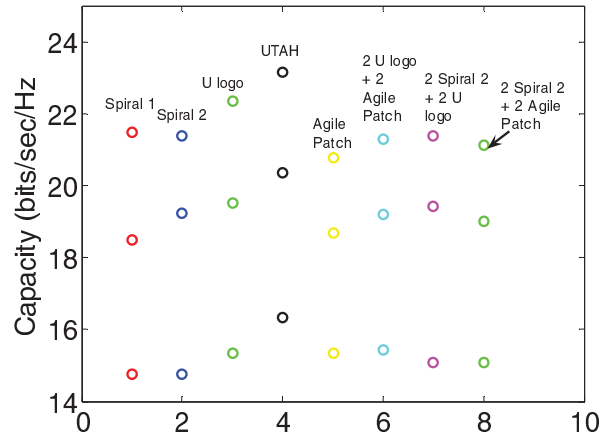


Figure 8: Capacity plot for the Rockwell T-39 channel simulated using the 3D ray-tracing model and assuming an SNR of 20 dB for receiver location Rx18-Rx34. Here we plot the capacity for the top 8 antennas selected from 1680 combinations.

For the antennas on the floor of the aircraft, the UTAH antenna provided optimum capacity, followed by the U logo antenna. Similar results were obtained when the optimizer was run on 1680 antenna combinations. It can also be observed that the antenna combination of spiral 2 and agile patch also provided good capacity. The advantage of spiral and the U logo antenna is their small size which would allow a greater number of these antenna types to be built on sensors which would further increase capacity. The results show that the higher the gain of the antenna, the higher is the capacity

## REFERENCES

- [1] Sai Ananthanarayanan, Alyssa Magleby Richards, and Cynthia Furse, "MIMO wireless communication for aircraft sensors," *12th Annual FAA/DOD/NASA Joint Aging Aircraft Conference*, Kansas City, MO, May 4-7, 2009
- [2] Sai Ananthanarayanan, Alyssa Magleby Richards, and Cynthia Furse, "Wireless and surface wave communication for aircraft sensor networks," *Aircraft, Airworthiness and Sustainment Conference*, Austin, TX, May 2010.
- [3] Alyssa Magleby, Cynthia Furse, Z. Q. Yun, "3D Ray Tracing for Intravehicle MIMO," *IEEE /URSI Antennas and Propagation Symposium*, Charleston, SC, June 1-5, 2009
- [4] S. Y. Lim, Z. Yun, J. M. Baker, N. Celik, H.-S. Youn, and M. F. Iskander "Radio Propagation in Stairwell: Measurement and Simulation Results." *IEEE Antennas and Propagation Society International Symposium*. Charleston, SC, 2009.
- [5] D. Landon, "Polarization misalignment and the design and analysis of compact multiple input multiple output arrays," Ph.D. Dissertation, University of Utah, 2007
- [6] M. A. Jensen and J. W. Wallace, "Review of antennas and propagation for MIMO wireless communications," *IEEE Trans. on Antennas and Propagation*, vol. 52, no. 11, November 2004, pp. 2810-2824